

## **PHOTOCATALYTIC STUDY USING La-Ag AND Ni-Ag DOPED COBALT OXIDE NANOPARTICLES AS PHOTOCATALYST**

S. Sivagami, Dr. K. Kalpanadevi\*

PG and Research Department of Chemistry, Kongunadu Arts and Science College, Coimbatore – 641 029

### **ABSTRACT**

The present work deals with the synthesis of La-Ag and Ni-Ag doped cobalt oxide nanoparticles, their characterization by FT-IR, XRD, SEM, TEM analyses and photo dye degradation study using the doped cobalt oxide NPs as catalyst. The study shows the efficacy of doped cobalt oxide NPs to degrade the dyes viz. Methyl Orange (MO) and Methylene Blue (MB) by irradiation with light. Considering unique band energy gaps associated with the nanostructured cobalt oxide NPs, the study deals with photo dye degradation efficiency of doped  $\text{Co}_3\text{O}_4$  NPs analyzed with UV-Vis spectroscopy. Following the synthesis of La-Ag doped  $\text{Co}_3\text{O}_4$  and Ni-Ag doped  $\text{Co}_3\text{O}_4$  NPs using thermal decomposition method, photo dye degradation study was carried out with varied time intervals.

**KEYWORDS:** UV-Vis spectra, Photo dye degradation, Methyl Orange (MO), Methylene Blue (MB).

### **INTRODUCTION**

In recent decades, globally facing problems with pollutants and contaminants by using different types of dyes as it discharges high content of organic and inorganic substances. About 800,000 tons per year production of worldwide in manufacturing industry, textile industry, etc. Untreated discharge of effluents from several manufacturing industries commonly contains synthetic dyes that harm the aquatic living [1,2]. Synthetic dyes which are used in industries show considerable diversity such as azo, anthrax quinone, sulphur, indigoid, triphenyl methyl (trityl), and phthalo cyanine derivatives [3]. The toxicity of dye that has chemical content can initiate substantial environmental pollution and serious health-risk factors [4]. Cobalt oxide nanoparticles have adequate band hole for the corruption of colours [5-8].

Photo degradation, a process in which a substance breaks down or undergoes structural changes under the influence of light, is a significant area of study with wide-ranging applications. In recent years, the integration of nanoparticles into this field has opened up new avenues for enhancing the efficiency and selectivity of photo degradation processes.

Nanoparticles, due to their unique size-dependent properties, have demonstrated remarkable potential in catalysing and accelerating photo degradation reactions [9].

The utilization of nanoparticles in photo degradation processes has gained considerable attention across various scientific disciplines, including environmental science, materials science, and nanotechnology. These nanoparticles, often tailored for specific applications, play a crucial role in promoting photo catalytic reactions, where light energy is harnessed to initiate chemical transformations. This introduction marks the convergence of two dynamic fields - nanotechnology and environmental science, highlighting the promising role of nanoparticles in advancing the understanding and application of photo degradation processes. As we move deeper into this synergy, we explore the mechanisms, challenges, and potential solutions associated with leveraging nanoparticles for enhanced photo degradation efficiency. Cobalt oxide nanoparticles have been investigated for their catalytic properties in various chemical reactions, including photocatalytic dye degradation. Hence, an attempt has been made to explore the photocatalytic dye degradation capability of La-Ag doped  $\text{Co}_3\text{O}_4$  and Ni-Ag doped  $\text{Co}_3\text{O}_4$  nanoparticles towards an azo dye (Methyl orange) and a thiazine dye (Methylene Blue).

## **EXPERIMENTATION**

### **Materials and Methods**

$\text{Co}(\text{NO}_3)_2 \cdot 6\text{H}_2\text{O}$ ,  $\text{Ni}(\text{NO}_3)_2 \cdot 6\text{H}_2\text{O}$ ,  $\text{AgNO}_3 \cdot 6\text{H}_2\text{O}$ ,  $\text{La}(\text{NO}_3)_3 \cdot 6\text{H}_2\text{O}$ , Phenyl acetic acid ( $\text{C}_6\text{H}_5\text{CH}_2\text{COOH}$ ), Hydrazine hydrate (99% and density-1.032 g/ml), Diethyl ether ( $(\text{CH}_3\text{CH}_2)_2\text{O}$ ), Carbon tetrachloride ( $\text{CCl}_4$ ), Conc. HCl, Potassium Iodate ( $\text{KIO}_3$ ) were purchased from Hi-media and used for the research work. All the chemicals used were of analytical grade and used without any further purification. Double deionised water was used throughout the work.

### **Chemical Synthesis of La-Ag doped and Ni-Ag doped Cobalt Oxide Nanoparticles**

Precursors were prepared using Co-precipitation method with cobalt nitrate with appropriate proportions of metal salts, phenyl acetic acid and hydrazine hydrate to obtain  $[(\text{La}_{0.2}\text{Ag}_{0.2}\text{Co}_{0.6}(\text{C}_6\text{H}_5\text{CH}_2\text{COO})_2(\text{N}_2\text{H}_4)_2)]$  and  $[(\text{Ni}_{0.2}\text{Ag}_{0.2}\text{Co}_{0.6}(\text{C}_6\text{H}_5\text{CH}_2\text{COO})_2(\text{N}_2\text{H}_4)_2)]$ . The obtained precursors were calcined using at about  $500^\circ\text{C}$ . The acquired black powdery substances were characterized by FT-IR, XRD, SEM, TEM and UV-Vis spectroscopy techniques.

## Physico-Chemical Techniques

FT-IR spectra of the calcined doped metal oxide samples were been recorded using SHIMADZU with pressed KBr pellets. X-ray patterns were recorded for the metal oxide NPs samples using X'pert Pro P analytical instrument. The calcined samples' morphological studies were done using FE-SEM analyzer (Zeiss-Gemini 300 SEM). Using SHIMADZU/206- 26300-48, UV-vis spectrophotometry along with photodegradation studies were carried out.

## RESULTS AND DISCUSSION

### FT-IR spectroscopy

FT-IR spectra of La-Ag doped  $\text{Co}_3\text{O}_4$  and Ni-Ag doped  $\text{Co}_3\text{O}_4$  nanoparticles are shown in **Figure 1**, which aids in understanding how doping affects the nanoparticle properties, like catalytic activity, electronic structure etc., In the FT-IR spectra of both the samples, two strong peaks appearing at  $658\text{ cm}^{-1}$  and  $558\text{ cm}^{-1}$  affirm the formation of a  $\text{Co}_3\text{O}_4$  spinel oxide associated with  $\text{Co}^{3+}$  in Octahedral site and  $\text{Co}^{2+}$  in tetrahedral site [10].

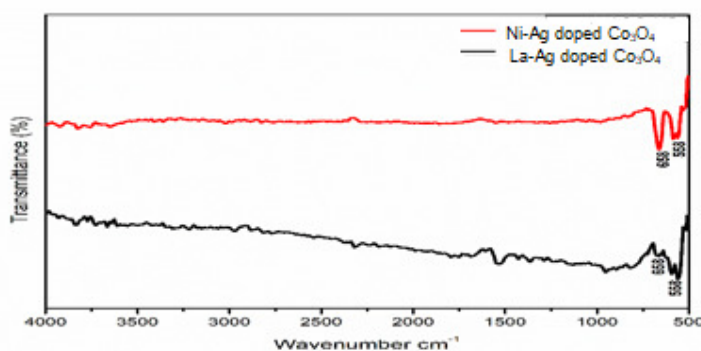


**Fig.1 - FT-IR spectra of La-Ag doped  $\text{Co}_3\text{O}_4$  and Ni-Ag doped  $\text{Co}_3\text{O}_4$  nanoparticles**

### XRD ANALYSIS

The XRD pattern of  $\text{Co}_3\text{O}_4$  shows (hkl) values at (111), (220), (311), (400), (511) and (440) at  $2\theta$  angles of  $23.34^\circ$ ,  $33.64^\circ$ ,  $41.00^\circ$ ,  $59.1^\circ$  and  $65.9^\circ$  respectively, which can be readily indexed to face centered cubic with  $Fd3m$  (JCPDS card No.80-1535) [11]. It can be observed from the XRD pattern that the doped Nickel, Silver and Lanthanum, Silver ions have been partially incorporated into the cobalt lattice sites without major distorting crystal symmetry.

The crystallite sizes of both the samples calculated from the Full Width at Half Maximum (FWHM) from their respective strongest peaks at (311) and (220) using Scherrer's equation,

$$D = K \lambda / \beta \cos \theta$$

where  $\lambda$  is the wavelength of X-ray,  $D$  is the average crystallite size,  $\beta$  is the FWHM,  $\theta$  represents the Bragg's angle at the corresponding peak and  $K$  is the instrumental constant, were found to fall in the range 11-14 nm.

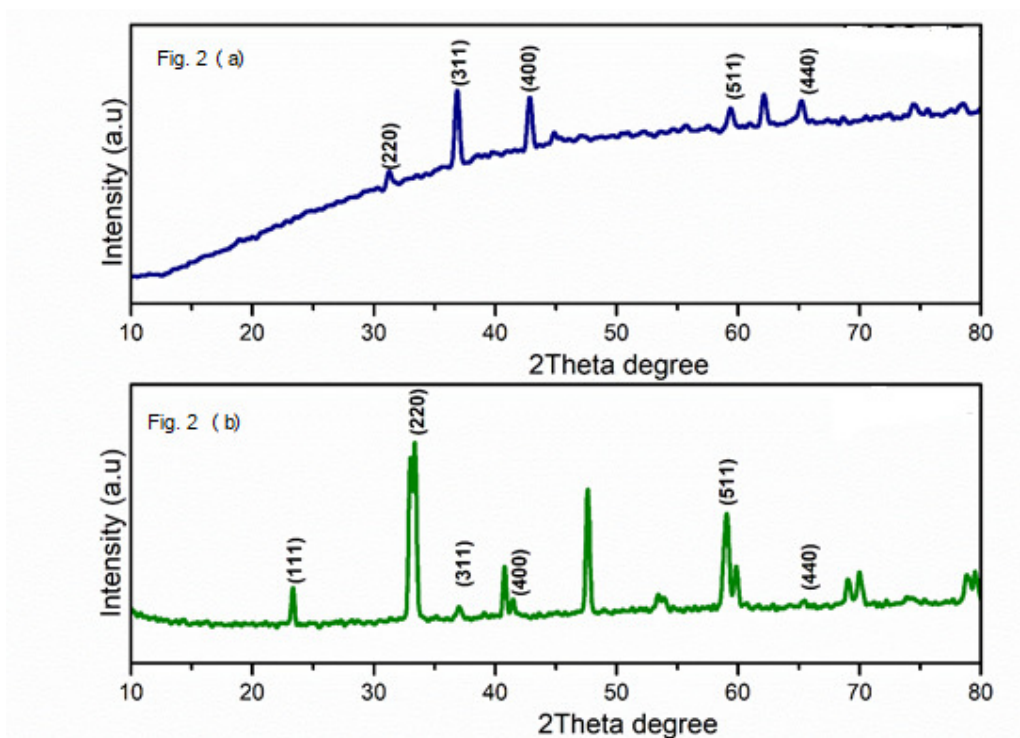


**Fig. 2 (a) - XRD Pattern of La-Ag doped Co<sub>3</sub>O<sub>4</sub> nanoparticles**

**Fig. 2 (b) - XRD Pattern of Ni-Ag doped Co<sub>3</sub>O<sub>4</sub> nanoparticles**

### SEM and EDAX Analyses

Figures 3a and 3b respectively show the morphology of La-Ag doped Co<sub>3</sub>O<sub>4</sub> and Ni-Ag doped Co<sub>3</sub>O<sub>4</sub> nanoparticles. Both the nanostructured samples are seemed to possess enhanced physico-chemical properties such as surface phenomena and catalytic stability. The nanoparticles appear to have angular, plate-like structures with sharp edges and corners. The particles remain clustered, forming larger agglomerates. This suggests a strong tendency for these particles to stick together, possibly due to van der Waals forces or other intermolecular interactions.

The EDAX spectra of both samples clearly demonstrate the presence of elements like Ni, Ag, Co and O, and La Ag, Co and O respectively. These results are consistent with the XRD patterns, implying the purity of the sample.

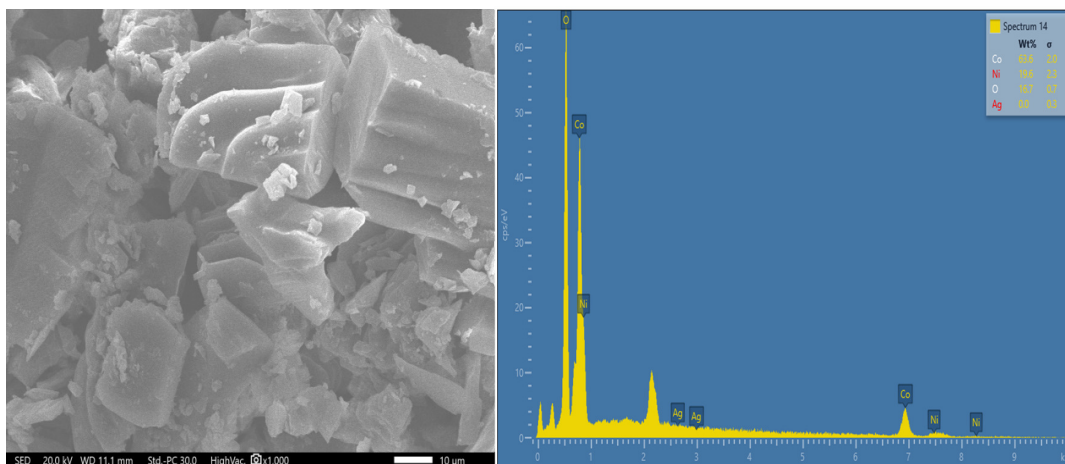


Fig (3a)

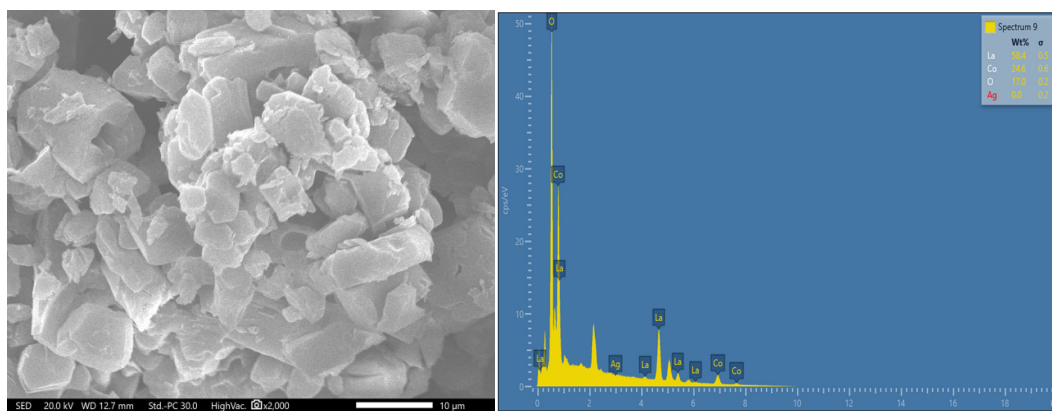
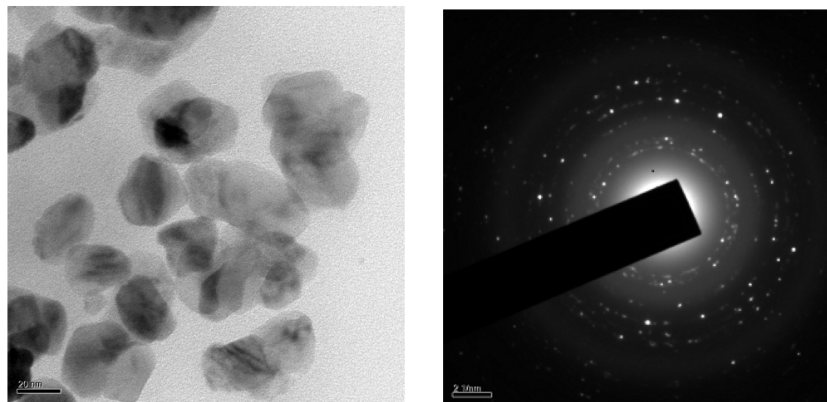


Fig (3b)

**Fig. (3a &3b) - SEM images and EDAX spectra of La-Ag doped  $\text{Co}_3\text{O}_4$  and Ni-Ag doped  $\text{Co}_3\text{O}_4$  nanoparticles**

### HRTEM Analysis

Figures 4 (a & b) show the HRTEM images and SAED patterns of La-Ag doped  $\text{Co}_3\text{O}_4$  and Ni-Ag doped  $\text{Co}_3\text{O}_4$  nanoparticles respectively. The presence of some bigger particles can be attributed to be the aggregation or overlapping of some small particles, due to their magnetic induction. The average grain size observed from the micrograph is about 11-13 nm, which is in agreement with the calculation using Scherrer's equation. Fig. 3.5 shows that the SAED pattern consists of sharp rings, which reveal the polycrystalline nature of the nanoparticles.



**Fig (4a)**

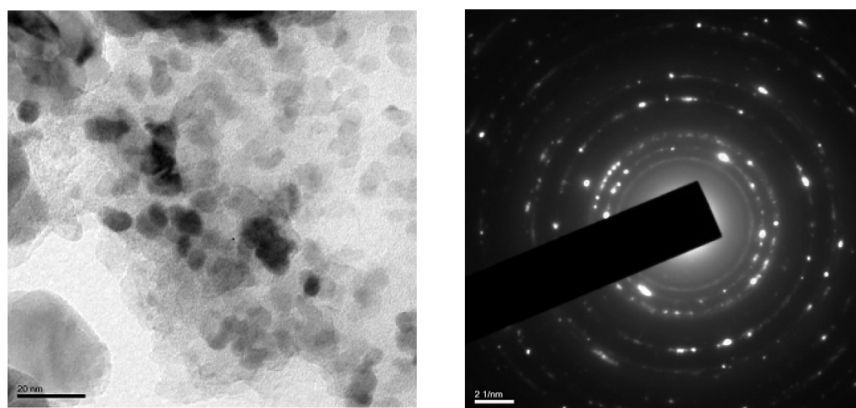


**Fig (4b)**

**Fig. (4a &4b) - HRTEM images and SAED patterns of La-Ag doped  $\text{Co}_3\text{O}_4$  and Ni-Ag doped  $\text{Co}_3\text{O}_4$  nanoparticles**

### **PHOTO CATALYTICAL STUDY**

The photo catalytic activity of the synthesized NPs has been investigated using Methyl Orange and Methylene Blue dye. A tremendous physical and chemical techniques like chlorination, ultra filtration, ozonation and coagulation helps degradation of dyes and secondary pollution issues are confronted [12].

The above said application was mostly prepared as bulk material using co-precipitation method [13-15]. The experiment was performed using freshly prepared MO and MB aqueous solution taking 5 mg/500 ml. Before the initiation of light irradiation, about 50 mg of synthesized catalyst was added to 100 ml freshly prepared dye solution. The catalyst solution is stirred for 45 min under dark using magnetic stirrer in order to attain the adsorption-desorption equilibrium. Subsequently, the solution was irradiated using 20W compact lamp

with 130 cd. The sample solution is collected with varied time interval of 0-75 min for every 15 min. The dye solutions MO and MB have the nature pH of 4.2 and 6.5 respectively. The absorbance values of MO were found to be at 460 nm and 463 nm for MO-La-Ag doped  $\text{Co}_3\text{O}_4$  and MO-Ni-Ag doped  $\text{Co}_3\text{O}_4$  respectively, while that of MB were found at 255 nm and 257 nm respectively for MB-La-Ag doped  $\text{Co}_3\text{O}_4$  and MB-Ni-Ag doped  $\text{Co}_3\text{O}_4$  respectively using UV-Vis spectrophotometer as shown in figures 4a, 4b, 4c and 4d.

To determine the photo catalytic efficiency of MO and MB, the following equation has been applied;

$$\text{Photo dye degradation \%} = \frac{C_0 - C}{C_0} \times 100$$

where  $C_0$  is the initial concentration of the dye and  $C$  is the concentration of the dye at time  $t$ . As it has been referred that photo catalytic property increases with the number of dopants is increased. In heterogeneous photocatalytic degradation, the efficiency is higher as the number of reactive oxygen sites is greater and the OH radicals than in single species.

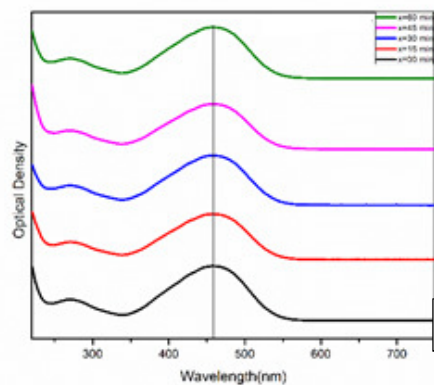


Fig:4a

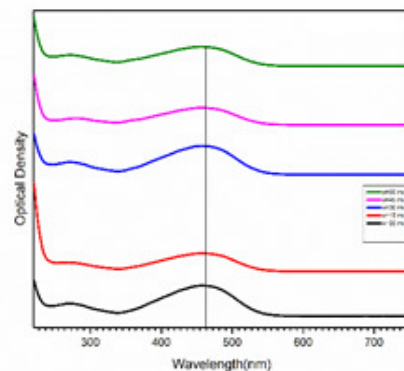


Fig.4b

**Fig. 4a - UV-vis absorption plot for MO-La-Ag doped  $\text{Co}_3\text{O}_4$  nanoparticles**

**Fig. 4b - UV-vis absorption plot for MO-Ni-Ag doped  $\text{Co}_3\text{O}_4$  nanoparticles**

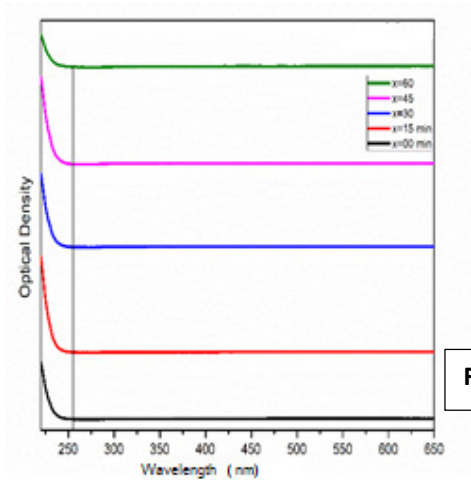


Fig:4c

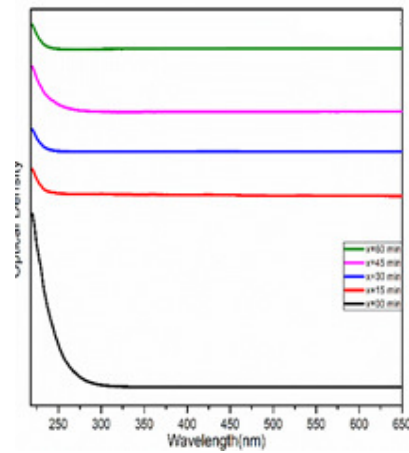


Fig: 4d

Fig. 4c - UV-vis absorbtion plot for MB-La-Ag doped  $\text{Co}_3\text{O}_4$  nanoparticles

Fig. 4d - UV-vis absorbtion plot for MB-Ni-Ag doped  $\text{Co}_3\text{O}_4$  nanoparticles

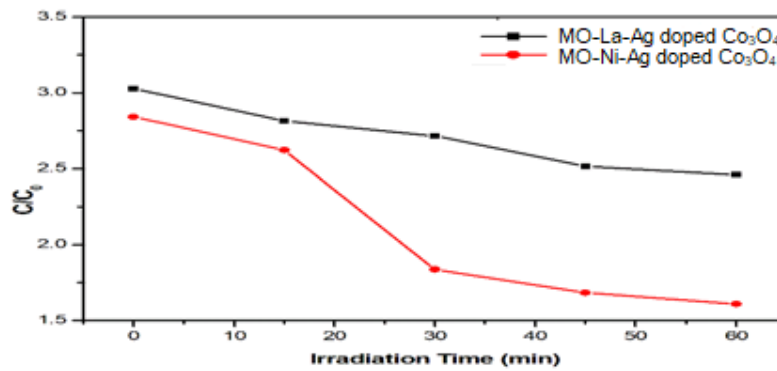


Fig. 5 Photo dye degradation of MO-La-Ag doped  $\text{Co}_3\text{O}_4$  and MO-Ni-Ag doped  $\text{Co}_3\text{O}_4$  nanoparticles

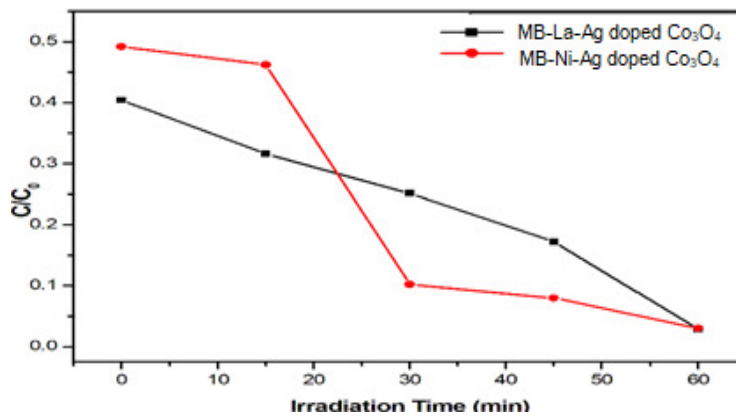


Fig: 6

Fig. 6 Photo dye degradation of MB-La-Ag doped  $\text{Co}_3\text{O}_4$  MB-Ni-Ag doped  $\text{Co}_3\text{O}_4$  nanoparticles



In MO-La-Ag doped  $\text{Co}_3\text{O}_4$ , the concentration ratio decreases gradually over time, starting at around 3.0 and reaching slightly above 2.5 at 60 minutes, whereas in MO-Ni-Ag doped  $\text{Co}_3\text{O}_4$ , the concentration ratio decreases more rapidly, starting at around 3.0 and reaching approximately 1.5 at 60 minutes. The former shows a faster and more significant reduction in concentration compared to the latter under the same irradiation conditions. This suggests that MO-La-Ag doped  $\text{Co}_3\text{O}_4$  are more effective in reducing the concentration over the given time period.

In MB-La-Ag doped  $\text{Co}_3\text{O}_4$ , the concentration ratio drops steadily over time, reaching approximately zero around 60 minutes, while in MB-Ni-Ag doped  $\text{Co}_3\text{O}_4$ , the concentration ratio decreases more quickly, reaching approximately zero around 50 minutes (Fig. 6). The MB-La-Ag doped  $\text{Co}_3\text{O}_4$  nanoparticles show a rapid reduction in concentration compared to MB-La-Ag doped  $\text{Co}_3\text{O}_4$  the under similar conditions. This implies that MB-Ni-Ag doped  $\text{Co}_3\text{O}_4$  nanoparticles are found to be more effectual in reducing the concentration over the given time period than that of MB-La-Ag doped  $\text{Co}_3\text{O}_4$  nanoparticles.

Moreover, the corresponding band gap energies of MO-La-Ag doped  $\text{Co}_3\text{O}_4$  and MO-Ni-Ag doped  $\text{Co}_3\text{O}_4$  nanoparticles and, MB-La-Ag doped  $\text{Co}_3\text{O}_4$  and MB-Ni-Ag doped  $\text{Co}_3\text{O}_4$  nanoparticles were calculated as 5.3eV, 5.2eV and 5.3eV, 5.1eV respectively using Tauc's formula as shown in Fig.7.

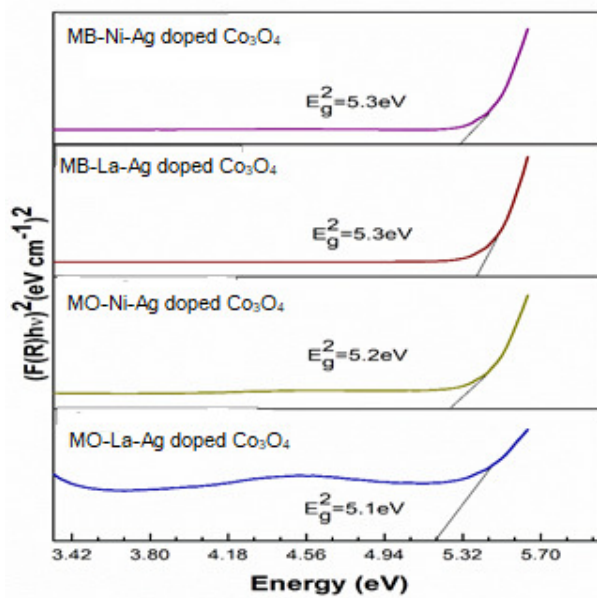


**Fig. 7-Tauc Plot of Methyl Orange and Methylene Blue dye with La-Ag doped  $\text{Co}_3\text{O}_4$  and Ni-Ag doped  $\text{Co}_3\text{O}_4$  nanoparticles**

## CONCLUSIONS

In brief, La-Ag doped  $\text{Co}_3\text{O}_4$  and Ni-Ag doped  $\text{Co}_3\text{O}_4$  nanoparticles were synthesized using thermal decomposition method. XRD studies affirmed the presence of nanoparticles of size varying from 11-14 nm in both samples, which was in agreement with the HRTEM results as well. SEM images of both the samples showed plate-like structures. The UV absorption depicted the shifts in the bandgap due to the non-uniform size of the nanoparticles. The photocatalytic activities of the samples towards Methyl Orange and Methylene Blue dye showed noticeable degradation in short period of time.

## ACKNOWLEDGEMENT

The authors are grateful to Kongunadu Arts and Science College, Coimbatore for providing required facilities for the synthesis of the material. Also, the authors wish to thank CNR-LAB, Avinashilingam Institute for Home Science and Higher Education for Women Coimbatore, for providing instrumentation facilities.

## REFERENCES

- [1] C.A. Fewson, *Biotechnology* 6, 148–153 (1988).
- [2] S. Seshadri, P.L. Bishop, A.M. Agha, *Waste Manage.* 15, 127–137 (1994).
- [3] Forgacs, E., Cserháti, T., Orosb, G. *Journal of International Environment* 30, 953-971 (2004).
- [4] X. Yu, Q. Ji, J. Zhang, Z. Nie, Z. Liu, L. Wang, *Earth Environ. Sci.* 81, 209– 218, (2017).
- [5] Azhdari, F., Ghaz, M.M.: Photocatalytic degradation of textile dye direct orange 26 by using  $\text{CoFe}_2\text{O}_4/\text{Ag}_2\text{O}$ . *Adv Environ Technol* 2, 77–84 (2016).
- [6] El-Bahy, Z.M., Mohamed, M.M., Zidan, F.I., Thabet, M.S.: Photodegradation of acid green dye over Co–ZSM-5 catalysts prepared by incipient wetness impregnation technique. *J Hazard Mater* 153, 364–371 (2008).
- [7] Narde, S.B., Lanjewar, R.B., Gadegone, S.M., Lanjewar, M.R.: Photocatalytic degradation of azo dye congo red using  $\text{Ni}_{0.6}\text{Co}_{0.4}\text{Fe}_2\text{O}_4$  as photocatalyst. *Der Pharma Chem* 9(7), 115–120 (2017).
- [8] Sharma, O., Sharma, M.K.: Use of cobalt hexacyanoferrate (II) semiconductor in photocatalytic degradation of neutral red dye. *Int J ChemTech Res* 5(4), 1615–1622 (2013).

- [9] J. Iqbal, T. Jan, S. Ul-Hassan, I. Ahmed, Q. Mansoor, M.U. Ali, F. Abbas, M. Ismail. *AIP Adv.*, 5, 127112 (2015).
- [10] H. Shindy, *Basics in colors, dyes and pigments chemistry: A review. Chem. Int* 2(29), 2016 (2016).
- [11] M. Ghiasi, A. Malekzadeh, H. Mardani, Synthesis and optical properties of cubic Co<sub>3</sub>O<sub>4</sub> nanoparticles via thermal treatment of a trinuclear cobalt complex. *Mater. Sci. Semicond. Process.* 42, 311–318 (2016).
- [12] K. Xu, Yu. Xing, W. Zhao, W. Zeng, Density-dependent of gas-sensing properties of Co<sub>3</sub>O<sub>4</sub> nanowire arrays. *Physica E* 118, 113956 (2020).
- [13] K. Telmani, H. Lahmar, M. Benamira, L. Messaadia, M. Trari, Synthesis, optical and photo-electrochemical properties of NiBi<sub>2</sub>O<sub>4</sub> and its photocatalytic activity under solar light irradiation. *Optik* 207, 163762 (2020).
- [14] R. Itteboina, T.K. Sau, Sol-gel synthesis and characterizations of morphology-controlled Co<sub>3</sub>O<sub>4</sub> particles. *Materials Today: Proceedings* 9, 458–467 (2019).
- [15] R. Saravan, M. Sukhin, S.M. Muthukumar, M. Mubashera, P.V. Abinaya, R.P. Prasath, F. Mohammad, Won Chun Oh, and Suresh Sagadevan Evaluation of the photocatalytic efficiency of cobalt oxide nanoparticles towards the degradation of crystal violet and methylene violet dyes. *Optik* 207, 164428 (2020).